J|A|C|S
ARTICLES
Published on Web 08/29/2007

Time-Resolved Studies of Water Dynamics and Proton Transfer at the Alumina−Air Interface

Sophie Le Caër,*,† D. Jason Palmer,‡ Manuela Lima,‡ Jean Philippe Renault,† Georges Vigneron,† Roberto Righini,‡ and Stanislas Pommeret†

Contribution from Laboratoire Claude Fréjacques, CEA/Saclay, DSM/DRECAM/SCM, URA 331 CNRS, F-91191 Gif-sur-Yvette Cedex, France, and Polo Scientifico, University of Florence, Via Nello Carrara 1, I-50019 Sesto Fiorentino, Italy

Received January 3, 2007; E-mail: sophie.le-caer@cea.fr

Abstract: The present study aims to understand the dynamical properties of water and OH groups layered on an alumina surface mainly by means of femtosecond IR-pump IR-probe transient absorption spectroscopy. The experimental results obtained demonstrate the existence of several kinds of O−H vibrators on the surface of alumina membranes, distinguishing them by their behavior on the femtosecond time scale and by the anisotropy of their spectral response. In the high-frequency region (>3400 cm^{-1}), the absorption is due to well-packed aluminol groups and to physisorbed water patches on the surface. When pumping at 3200 cm^{-1}, physisorbed water hydrogen-bonded to $AlOH_2^+$ groups is observed. The anisotropy measurements demonstrate the existence of an efficient energy-transfer mechanism among the water molecules characterized by a time constant of 400 ± 100 fs. The persisting anisotropy at long times, especially in the case of AlOH groups and of the structured physisorbed water layer on top of them, proves the anisotropic structuring induced by the surface. The excitation at 3000 cm^{-1} enables the detection of a photon-induced proton-transfer reaction. The proton back-transfer reaction time constant is 350 ± 50 fs. From anisotropy measurements, we estimate the proton hopping time to be 900 ± 100 fs in a locally extended water network lying on the surface.

Introduction

In heterogeneous catalysis, the surface chemistry of the catalyst plays a key role in determining its performance.[1] Alumina (Al_2O_3) is a well-known catalyst[2] and is used as an industrial acid−base catalyst[3] (dehydration of alcohols,[4] isomerization[5]) as well as a metallic catalyst support.[6] In all these reactions, the OH coverage of alumina is of great importance, as it is known that the adsorption and catalytic properties of γ-alumina are directly associated with the state of its hydroxyl coverage.[7] However, although many experimental studies using infrared (IR)[3,8−10] spectroscopy and nuclear magnetic resonance (NMR)[11] have been performed to characterize surface hydroxyl groups, the signals obtained are very complex and the assignment of OH bands still remains controversial. Moreover, the simultaneous presence of molecular water and surface hydroxyl groups is a major obstacle to the understanding of the surface properties of alumina.

The behavior of water at interfaces is poorly understood compared to its behavior in neat liquid.[12] However, the understanding of its dynamical properties at interfaces is of crucial importance for heterogeneous catalysis, chemistry, biology, and environmental sciences.[13] The dynamical properties at the surface of nanoparticles have been studied by means of different experimental techniques, for example, time-resolved fluorescence-upconversion spectroscopy;[14] the dynamics of liquids confined in nanopores has been investigated with dielectric spectroscopy,[15] optical Kerr effect,[16] Raman spec-

† CEA/Saclay.
‡ University of Florence.

(1) Bell, A. T. *Science* **2003**, *299*, 1688.
(2) Hass, K. C.; Schneider, W. F.; Curioni, A.; Andreoni, W. *Science* **1998**, *282*, 265.
(3) Knözinger, H.; Ratnasamy, P. *Catal. Rev.−Sci. Eng.* **1978**, *17*, 31.
(4) (a) Pines, H.; Pillai, C. N. *J. Am. Chem. Soc.* **1961**, *83*, 3270. (b) Pillai, C. N.; Pines, H. *J. Am. Chem. Soc.* **1961**, *83*, 3274.
(5) (a) Hightower, J. W.; Hall, W. K. *J. Catal.* **1969**, *13*, 161. (b) Hightower, J. W.; Hall, W. K. *Trans. Faraday Soc.* **1970**, *66*, 477.
(6) (a) Furlong, B. K.; Hightower, J. W.; Chan, T. Y.-L.; Sarkany, A.; Guczi, L. *Appl. Catal., A* **1994**, *117*, 41. (b) Kaushik, V. K.; Sivaraj, C.; Rao, P. K. *Appl. Surf. Sci.* **1991**, *51*, 27.
(7) (a) Baumgarten, E.; Denecke, E. *J. Catal.* **1985**, *95*, 296. (b) Baumgarten, E.; Denecke, E. *J. Catal.* **1986**, *100*, 377. (c) Vlaev, L.; Damyanov, D.; Mohamed, M. M. *Colloids Surf.* **1989**, *36*, 427.
(8) (a) Peri, J. B.; Hannan, R. B. *J. Phys. Chem.* **1960**, *64*, 1526. (b) Peri, J. B. *J. Phys. Chem.* **1965**, *69*, 211. (c) Peri, J. B. *J. Phys. Chem.* **1965**, *69*, 220. (d) Dillon, A. C.; Ott, A. W.; Way, J. D.; George, S. M. *Surf. Sci.* **1995**, *322*, 230. (e) Morterra, C.; Magnacca, G. *Catal. Today* **1996**, *27*, 497.
(9) Tsyganenko, A. A.; Filimonov, V. N. *J. Mol. Struct.* **1973**, *19*, 579.
(10) Busca, G.; Lorenzelli, V.; Sanchez Escribano, V.; Guidetti, R. *J. Catal.* **1991**, *131*, 167.
(11) (a) Huggins, B. A.; Ellis, P. D. *J. Am. Chem. Soc.* **1992**, *114*, 2098. (b) Hietala, J.; Root, A.; Knuuttila, P. *J. Catal.* **1994**, *150*, 43.
(12) (a) Gale, G. M.; Gallot, G.; Hache, F.; Lascoux, N.; Bratos, S.; Leicknam, J. C. *Phys. Rev. Lett.* **1999**, *82*, 1068. (b) Gallot, G.; Bratos, S.; Pommeret, S.; Lascoux, N.; Leicknam, J. C.; Kozinski, M.; Amir, W.; Gale, G. M. *J. Chem. Phys.* **2002**, *117*, 11301. (c) Nibbering, E. T. J.; Elsaesser, T. *Chem. Rev.* **2004**, *104*, 1887. (d) Laage, D.; Hynes, J. T. *Science* **2006**, *311*, 832. (e) Eaves, J. D.; Loparo, J. J.; Fecko, C. J.; Roberts, S. T.; Tokmakoff, A.; Geissler, P. L. *Proc. Natl. Acad. Sci. U.S.A.* **2005**, *102*, 13019.
(13) (a) Tan, H.-S.; Piletic, I. R.; Fayer, M. D. *J. Chem. Phys.* **2005**, *122*, 174501. (b) Le Caër, S.; Rotureau, P.; Brunet, F.; Charpentier, T.; Blain, G.; Renault, J. P.; Mialocq, J.-C. *ChemPhysChem* **2005**, *6*, 2585.
(14) Pant, D.; Levinger, N. E. *J. Phys. Chem. B* **1999**, *103*, 7846.
(15) Nandi, N.; Bhattacharyya, K.; Bagchi, B. *Chem. Rev.* **2000**, *100*, 2013.

10.1021/ja0691730 CCC: $37.00

troscopy, dynamic light scattering, neutron scattering,[17] and so forth. Moreover, sum-frequency vibrational spectroscopy[18] and quasi-elastic neutron scattering[19] have proven to be efficient tools to study surfaces. Among these techniques, ultrafast infrared−infrared (IR−IR) pump−probe spectroscopy[20] is a very powerful tool enabling direct access to the dynamical properties of water in nanomaterials.

The complexity of the interpretation of the different components present in mid-IR spectra of water on alumina surfaces is because water readily adsorbs to the surface as molecular water or dissociates to form hydroxyl groups on the surface; these groups are capable of hydrogen bonding. The position of the absorption bands of OH groups participating in the formation of hydrogen bonds is determined by the strength of these bonds, depending on the relative difference in their acid and base properties, the distance between the groups, their mutual interactions, and so forth. Furthermore, the O−H groups can occupy different types of sites on the surface. For example, the adsorption sites (the aluminum ion can occupy a tetrahedral or octahedral site in γ-alumina) and the number of neighboring hydroxyl groups influence the acidity and the OH stretching frequency.[3] Several types of catalytic sites are present on the alumina surface, including Brønsted acid, Lewis acid, and Lewis base sites, leading to a complex characterization of the surface's acidity. The different acid sites on the surface are in general understood using experiments with different probe molecules.[8e]

The present article deals with dynamical properties of water and aluminol groups in nanoporous γ-alumina using the OH stretching vibration as a probe of dynamics. The aims are to measure the lifetime of the first vibrational excited state of the OH vibrator and to gain some information on the dynamics of water at an interface. Thus, we have performed anisotropy experiments that measure the rapid energy-transfer processes in water.[12b]

Experimental Section

Nanoporous γ-Alumina. Alumina can exist in several phases, all of which consist of a close-packed oxygen lattice in which the aluminum cations occupy the tetrahedral and/or octahedral vacancies. We worked with the γ-phase of alumina. Neutron diffraction data showed that γ-Al_2O_3 has a spinel-like structure in which octahedral and tetrahedral aluminum ions are randomly distributed in such a way that 10% of tetrahedral and 46.7% of octahedral sites are occupied.[21a] In other words, the aluminum cations occupy both some tetrahedral and octahedral vacancies in a face-centered cubic oxygen sublattice.[21b]

Alumina membranes[22] (Anodisc aluminum oxide membrane filters, Whatman International) used here were 47 mm in diameter with 200-nm pore diameters, 60-μm thick, and they had a porosity of ~30%. The pores are arranged in a honeycomb-type morphology.[23] The specific area is small, ~6 m^2/g.[23]

FT-IR Spectrum. IR measurements were performed at room temperature and under ambient atmosphere at a 4 cm^{-1} resolution using a Bruker Vertex 70.

Nonlinear Infrared Experiments: Infrared−Infrared Pump−Probe Experimental Setup.[24] The infrared laser source for the experiments is based on a commercial Ti:sapphire oscillator and amplifier system (Thales Laser). The output is a 1 kHz train of 600-μJ pulses at 800 nm. This output is evenly split between two different optical parametric amplifier (OPA) systems. In both cases, the infrared output is on the order of 1 μJ with a spectral width of ~200 cm^{-1} and a temporal width of approximately 100 fs. The pump radiation for the pump−probe experiments is generated in a TOPAS (Light Conversion Ltd.). The probe and reference beams are produced in a home-built OPA[25] and are attenuated and spatially separated by means of reflection from the two faces of a wedged CaF_2 plate. The pump beam passes through a half-wave plate to control the polarization relative to that of the probe and then traverses a variable delay line. The probe and reference beam polarizations remain fixed. The pump, probe, and reference beams are focused into the sample with parabolic mirrors, and the probe and reference beams are then imaged into a monochromator (TRIAX 180, HORIBA Jobin Yvon) and dispersed onto two 32-channel arrays of a liquid nitrogen-cooled mercury cadmium telluride (MCT) detector (InfraRed Associates Inc.). The MCT response and accuracy of the measured intensity were carefully tested using a series of experiments on test chromophores in solution which gave the exact value of anisotropy (0.4) as predicted by theory. The pump beam is chopped at half the laser repetition rate to eliminate the effects of long-term laser drift. Acquisition software determines the ratio of the pump on−pump off probe intensity, normalized to the reference beam intensity, yielding a transient absorption signal that is recorded as a function of the pump−probe time delay. We used three different pumping frequencies at 3460, 3200, and 3000 cm^{-1}. The probed region ranged from 2900 to 3600 cm^{-1}, enabling a global picture of the H bond dynamics on the surface of alumina. We checked every day that the FT-IR spectrum of the sample was fully reproducible, thus indicating that the water coverage was the same for all experiments. The measured samples comprised a stack of three discs, yielding an optical density of roughly 0.5 at 3400 cm^{-1}. Because of the spectral width of the pump (200 cm^{-1}), the pump was not necessarily exciting a well-defined OH species on the surface. Instead, the frequency bandwidth of the pump is of the same order as the spectral bandwidth of the absorbing species.

Anisotropy. The anisotropy data were calculated from the spectrally resolved transient kinetics using the following procedure. Instead of calculating the anisotropy for each frequency of the probe beam (32 channels over 200 cm^{-1}), we first calculated the mean transient absorption (parallel and perpendicular polarizations) for each pump frequency (the mean value of the transient optical density over the 32 channels) and then calculated the anisotropy of this mean transient absorption. To extract the fast dynamics of the anisotropy, we have developed a procedure that is described in section II in the Supporting Information.

Fitting Procedure. The kinetics were fitted as a sum of Dirac (instantaneous contribution), exponential (vibrational relaxation), and Heaviside functions (long-lived contributions); for more details, see section II in the Supporting Information. The fit was optimized according to the least-square method using the Levenberg−Marquardt method.[26] The eventual interdependency of the parameters of the fit was checked by changing randomly the value of the parameters and then injecting that new set of parameters as a new guess for the initial parameters of the fit. This operation was typically performed more than 1000 times. The results of those 1000 fits were used to estimate the

(16) Scodinu, A.; Fourkas, J. T. *J. Phys. Chem. B* **2002**, *106*, 10292.
(17) Crupi, V.; Majolino, D.; Migliardo, P.; Venuti, V. *J. Phys. Chem. A* **2000**, *104*, 11000.
(18) (a) Du, Q.; Freysz, E.; Shen, Y. R. *Phys. Rev. Lett.* **1994**, *72*, 238. (b) Eisenthal, K. B. *Chem. Rev.* **1996**, *96*, 1343. (c) Ostroverkhov, V.; Waychunas, G. A.; Shen, Y. R. *Chem. Phys. Lett.* **2004**, *386*, 144. (d) Ueba, H.; Wolf, M. *Science* **2005**, *310*, 1774.
(19) Mamontov, E. *J. Chem. Phys.* **2004**, *121*, 9087.
(20) (a) Heilweil, E. J.; Casassa, M. P.; Cavanagh, R. R.; Stephenson, J. C. *Annu. Rev. Phys. Chem.* **1989**, *40*, 143. (b) Onda, K.; Tanabe, K.; Noguchi, H.; Wada, A.; Shido, T.; Yamaguchi, A.; Iwasawa, Y. *J. Phys. Chem. B* **2001**, *105*, 11456.
(21) (a) Verwey, E. J. W. *Z. Kristallogr.* **1935**, *91*, 317. (b) Cai, S. H.; Rashkeev, S. N.; Pantelides, S. T.; Sohlberg, K. *Phys. Rev. Lett.* **2002**, *89*, 235501.
(22) (a) Furneaux, R. C.; Rigby, W. R.; Davidson, A. P. *Nature* **1989**, *337*, 147. (b) Li, F.; Zhang, L.; Metzger, R. M. *Chem. Mater.* **1998**, *10*, 2470.
(23) Crawford, G. P.; Steele, L. M.; Ondris-Crawford, R.; Iannacchione, G. S.; Yeager, C. J.; Doane, J. W.; Finotello, D. *J. Chem. Phys.* **1992**, *96*, 7788.
(24) Hamm, P.; Lim, M.; Hochstrasser, R. M. *J. Phys. Chem. B* **1998**, *102*, 6123.
(25) Hamm, P.; Kaindl, R. A.; Stenger, J. *Opt. Lett.* **2000**, *25*, 1798.
(26) Press, W. H.; Flannery, B. P.; Teukolsky, S. A.; Vetterling, W. T. *Numerical Recipes in C: The Art of Scientific Computing;* Cambridge University Press: Cambridge, 1988−1992.

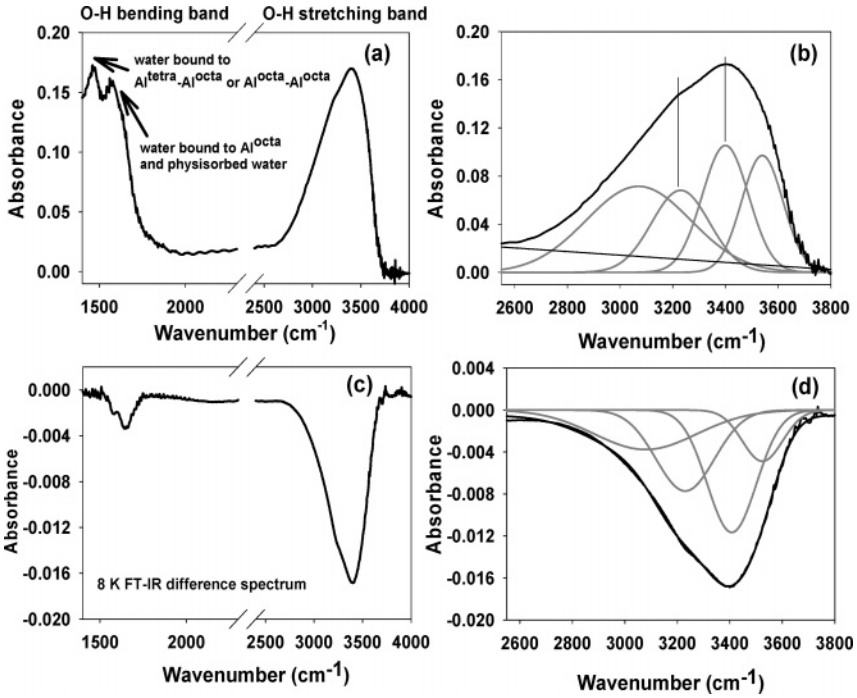

Figure 1. (a) FT-IR spectra in the 1400−4000 cm^{-1} spectra domain for a 200-nm Anodisc aluminum oxide membrane filter at room temperature (295 K) and atmospheric pressure, the reference being air. (b) Fit of the OH stretching band obtained in (a). The experimental and fitted points are represented with the black lines; they correspond nicely. Four bands (gray lines) are necessary to obtain this good agreement. The baseline is represented with the thin black line. The lines indicate typical points in the FT-IR spectrum that determine the values of two maxima: 3410 and 3220 cm^{-1}. The two other bands are found to have a maximum at 3530 cm^{-1} (in agreement with the literature[3]) and at 3080 cm^{-1}. The maximum values are determined with an error bar of 20 cm^{-1}. (c) Differential FT-IR spectrum obtained after heating at 303 K, the reference being the alumina at 295 K. (d) Fit of the band obtained in (c). The experimental and fitted points are represented with the black lines and are in good agreement. The same bands as those in (b) are used (gray lines) for this fitting procedure. The baseline is not represented. In all these spectra, the noise appearing for frequencies greater than 3600 cm^{-1} arises from water vapor.

errors on the parameters and their eventual interdependency. We found no interdependency in any of the results presented here. Unless otherwise specified, the time constants are determined within error bars of 15%.

Results and Discussion

Nanoporous γ-Alumina IR Steady-State Absorption Spectrum. The FT-IR spectrum of the nanoporous alumina membrane is displayed in Figure 1a. The major infrared features are observed at 1145 (not shown), 1467, and 1566 cm^{-1} and in the 2600−3800 cm^{-1} region (Figure 1a). For frequencies lower than 1200 cm^{-1} (not shown), the sharp profile of the spectrum is due to the cutoff (ca. 1000 cm^{-1}) imposed by bulk alumina phonon modes.[27] The absorption bands located in the 1350−1600 cm^{-1} region are attributed to water molecules coordinatively bound to different unsaturated aluminum surface sites (namely, tetrahedral Al^{tetra} and octahedral Al^{octa} aluminum ions). The absorption band at 1566 cm^{-1} was attributed to the bending vibration of water molecules coordinated to octahedral aluminum ions, and the band at 1467 cm^{-1} to the bending vibration of water molecules coordinated to the pairs $Al^{tetra}-Al^{octa}$ and $Al^{octa}-Al^{octa}$, these two pairs of sites having close energies and being difficult to distinguish at high OH coverages.[7c] The species corresponding to these bands will be denoted hereafter as $AlOH_2^+$. The bending vibration of physisorbed H_2O around 1630−1650 cm^{-1} is also observed as a weak shoulder. The broad asymmetric infrared absorption feature in the 2800−3600 cm^{-1} region corresponds to the OH stretching band. The different components absorbing at frequencies greater than 3400 cm^{-1} are quite well understood in the literature,[3] whereas the species absorbing at lower frequencies have been less studied and the assignment of the components in this spectral region remains unclear. We fitted the OH stretching band as a sum of components centered, respectively, at 3530, 3410, 3220, and 3080 cm^{-1} (Figure 1b) with an error bar of 20 cm^{-1}.

To clarify the assignments of the different components, we performed FT-IR temperature difference spectra. Figure 1c depicts the case of heating at 303 K, the reference being the sample at ambient temperature (295 K). The FT-IR temperature difference spectrum obtained is then fitted using the species absorbing at 3530, 3410, 3220, and 3080 cm^{-1} (Figure 1d). The comparison between Figure 1b,d shows that the species located at low frequencies (3080 cm^{-1}) and at high frequencies (around 3530 cm^{-1}) are less affected by the heating than the species located at 3410 and 3220 cm^{-1}. These low and high frequencies can then be attributed to more strongly bound species (i.e., to chemisorbed species; see the area differences of the subbands in the fits plotted in Figure 1b,d). We checked that a gentle heating induces mainly the decrease of the components at 3410 and 3220 cm^{-1}, which disappear in a very similar manner and which can thus be attributed to physisorbed water. Moreover, the heating procedure induces a shift of the whole infrared spectrum in the 2600−4000 cm^{-1} region toward higher frequencies. For example, the broad peak centered at 3410 cm^{-1} in the case of the spectrum recorded at ambient temperature was detected around 3510 cm^{-1} after heating at 383 K, consistent with the loss of hydrogen bonds. Last, we checked, after heating at 383 K, that the absorption band at 1566 cm^{-1} had strongly

(27) Morterra, C.; Magnacca, G.; Cerrato, G.; Del Favero, N.; Filippi, F.; Folonari, C. V. *J. Chem. Soc., Faraday Trans.* **1993**, *89*, 135.

Scheme 1. OH Stretching Frequencies for Various OH Types on the Alumina Surface[a]

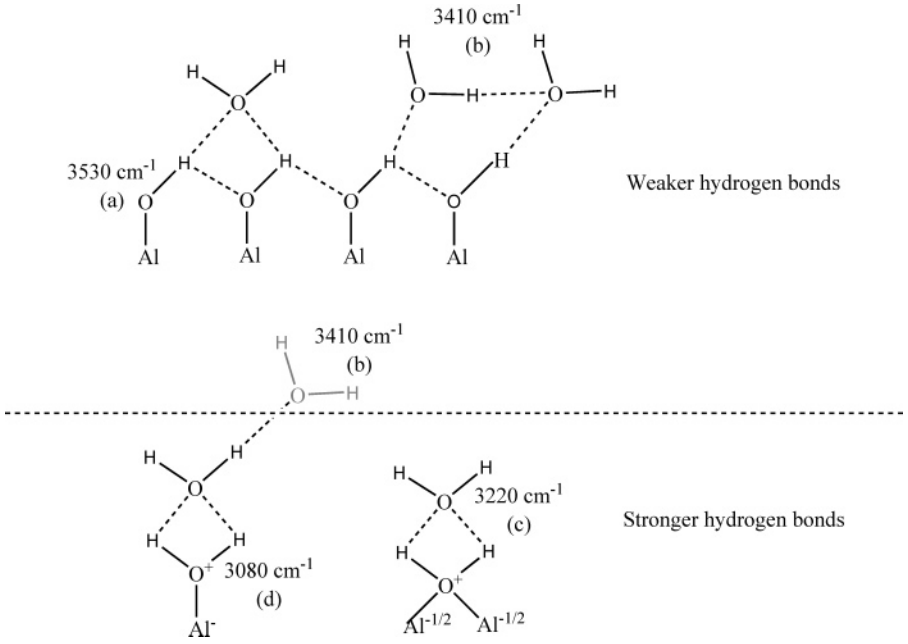

[a] Top: weak hydrogen bonds. Bottom: strong hydrogen bonds. The water molecule represented in gray on the bottom is weakly hydrogen-bonded. The dotted line separates weaker hydrogen bonds from stronger ones. The different bands are attributed to the following species: (a) hydrogen-bonded aluminols, (b) physisorbed water, (c) physisorbed water interacting with what we denote as $AlOH_2^+$ groups, (d) $AlOH_2^+$ acid sites.

decreased (mainly due to the loss of the 1650 cm^{-1} component corresponding to the bending mode of physisorbed water), whereas the absorption band at 1467 cm^{-1} had not changed (Figure 1c).

From literature data together with FT-IR temperature difference spectra, we draw the following conclusions (Scheme 1):

(a) The 3530 cm^{-1} band has been attributed to hydrogen-bonded alumina surface hydroxyls (AlO−H);[2,3]

(b) The 3410 cm^{-1} band is attributed to physisorbed water (namely the hydrogen-bonding network of adsorbed water). It corresponds to the main component removed at the lowest heating temperature. In addition, this component also has a contribution from hydrogen-bonded alumina surface hydroxyls.[3] It is worth pointing out that a frequency of 3475 cm^{-1} has been predicted for in-plane hydrogen-bonded OH groups of a fully hydroxylated alumina surface.[2] Thus, the O−H stretching vibration of aluminol groups can overlap with the molecularly adsorbed H_2O band;

(c) The 3220 cm^{-1} component corresponds to physisorbed water (as deduced from FT-IR temperature difference spectra), which is relatively strongly hydrogen bonded. As a matter of fact, the observed spectral shifts of the O−H stretching frequency are an indication of the strength or type of hydrogen bond: this frequency decreases when the hydrogen-bond energy increases. This contribution may thus be attributed to water in interaction with $AlOH_2^+$ sites on the surface (component d);

(d) The component at the lowest frequencies (3080 cm^{-1}) is due to chemisorbed species (Figure 1b). The chemisorbed species are undissociated water molecules and aluminol groups. These latter being component *a*, we can thus assign component *c* to undissociated water molecules mainly coordinated through the oxygen lone pair to the surface aluminum cations (octahedral aluminum ions and $Al^{tetra}-Al^{octa}$ and $Al^{octa}-Al^{octa}$ pairs). These groups are weak Brønsted acid sites on the surface. The acidity of the site leads to strong hydrogen bonds with surrounding water molecules and thus to this very low characteristic frequencies. Molecular orbital calculations[28] have shown that the O−H stretching in $AlOH_2^+$ is roughly 400−500 cm^{-1} lower in frequency than that of the O−H stretching in AlOH.

Thermal Gravimetric Analysis. Thermal gravimetric analysis (TGA) measurements in the 300−473 K temperature range evidence a small total weight loss of 0.4%. No weight loss is observed in the 473−873 K temperature range. The analysis was repeated after the full recovery of the initial weight by the sample stored under ambient atmosphere, and the same weight loss was determined. This reversible weight loss can be attributed to physisorbed water. The water content is then 0.0232 mol of water per mole of Al_2O_3. Knowing the specific area (6 m^2/g), we can deduce that there are 22 water molecules per nm^2 of the surface. Assuming that around 19 H_2O molecules fully cover a nm^2 of γ-alumina,[29] we conclude that there is roughly one layer of physisorbed water on the surface. Thus, there is a hydrogen-bonded water layer on top of the surface hydroxyl layer. This result is consistent with a previous FT-IR investigation on the (0001) α-alumina surface under different humidity conditions, proving that molecularly adsorbed H_2O can form a structured overlayer when the humidity is in the 10−70% range.[30] Al-Abadleh and Grassian[30] have also shown that a quasi-liquid layer is formed when humidity is higher than 70%. Under our conditions, the humidity is ∼50%. This humidity is consistent with the presence of a structured overlayer on top of the surface hydroxyl layer.

Having satisfactorily identified the species contributing to the broad OH stretching band, the purpose of our study is to

(28) Kubicki, J. D.; Blake, G. A.; Apitz, S. E. *Am. Mineral.* **1996**, *81*, 789.
(29) (a) McHale, J. M.; Auroux, A.; Perrotta, A. J.; Navrotsky, A. *Science* **1997**, *277*, 788. (b) McHale, J. M.; Navrotsky, A.; Perrotta, A. J. *J. Phys. Chem. B* **1997**, *101*, 603.
(30) Al-Abadleh, H. A.; Grassian, V. H. *Langmuir* **2003**, *19*, 341.

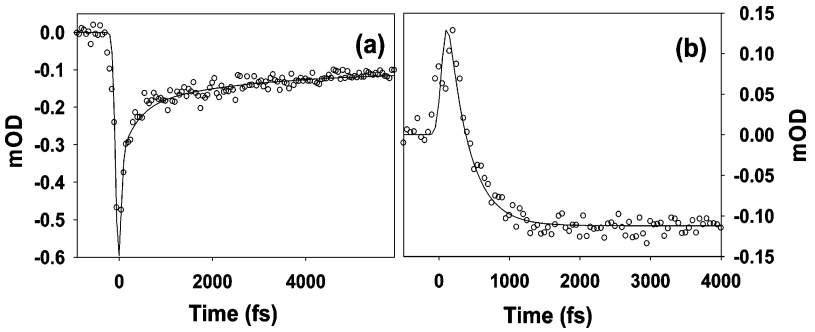

Figure 2. Typical examples of the transient absorption kinetics (symbols) and the fits (lines). (a) For a 3000 cm^{-1} pump and a 3177 cm^{-1} probe. (b) For a 3200 cm^{-1} pump and a 3026 cm^{-1} probe. Pump and probe have parallel polarizations, and the kinetics presented correspond to a single channel of the detector.

investigate its behavior by means of infrared−infrared pump−probe experiments to track these OH vibrators on the γ-alumina surface.

Femtosecond Results. The experimental transient absorption kinetics (Figure 2) were fitted using a global model with four contributions (eq 5 in section II in the Supporting Information): a coherent contribution when the pump and the probe pulses significantly overlap (instantaneous); a dominating fast contribution (350 fs); a marginal slow contribution (2.5 ps), and a Heaviside contribution. It is important to note that it was impossible to fit the data with a single exponential over the whole spectral range, regardless of pump frequency. We then chose to fit the decay of the induced absorption using two decay time constants (350 fs and 2.5 ps). The values of those time constants did not present any pump- and probe-frequency dependence. The nonmonoexponential decay may be attributed to the wide variety of OH sites on the alumina surface. Nevertheless, the mean lifetime of the induced absorption is well represented by the fast decay time (350 fs) since the 2.5-ps component plays a significant role only in the spectral regions where the transient absorption is small.

The Heaviside contribution highlights the fact that the system does not relax into its initial state on the time scale studied here (a few picoseconds) because of the temperature increase caused by the absorption of the intense pump pulse (the diffusion of the heat occurring out of the time window of the experiment). This has been discussed in the literature in the case of bulk water[31] and compared to temperature difference FT-IR spectra.[31a] The procedure to subtract both the coherent and the thermal contributions is provided in section II in the Supporting Information. Figure 3 presents the amplitude of the thermal contribution for a pump at 3000 cm^{-1} (the evolution being similar in the case of a pump at 3200 and 3460 cm^{-1}) together with a temperature difference FT-IR spectrum in the case of a heating temperature of 303 K. The transient absorption spectrum at long times shows features similar to the 8 K temperature difference FT-IR spectrum and is in agreement with a temperature increase of the sample induced by the pump. We note that a temperature increase of 2 K was estimated in HOD/H_2O liquid samples;[31a] nevertheless, in this case, the temperature difference FT-IR and the pump−probe spectrum are the same. In our case, the difference between the two spectra arises from thermodynamics. As a matter of fact, in the FT-IR difference

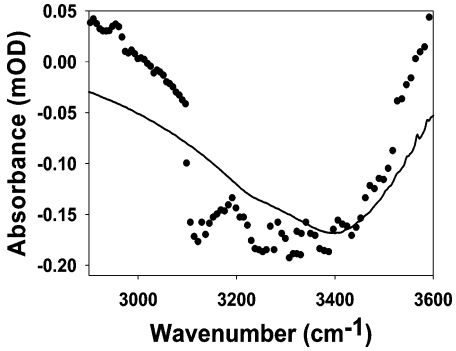

Figure 3. Comparison in the 2900−3600 cm^{-1} region between the thermal contribution (●) for a pump at 3000 cm^{-1} (similar results are obtained when pumping at 3200 and 3460 cm^{-1}; in all these cases, the pump and the probe have parallel polarizations) and the temperature difference FT-IR spectrum (black line) obtained for a 303 K heating, the reference being the sample at 295 K. To allow a better comparison, the FT-IR spectrum was divided by 100.

spectrum, which was recorded on a time scale of a few minutes, the equilibration between water at the alumina−air interface and in the gas phase takes place. That is evidently not the case on a time scale of a few picoseconds.

The anisotropy is defined as follows: $R = (\Delta\alpha_{\parallel} - \Delta\alpha_{\perp})/(\Delta\alpha_{\parallel} + 2\Delta\alpha_{\perp})$, where $\Delta\alpha_{\parallel}$ and $\Delta\alpha_{\perp}$ are the absorption changes measured with probe pulses that have parallel and perpendicular polarization with respect to the one of the pump, respectively. The anisotropy decay gives information on the reorientation of the dipole moment by rotational motions and/or energy transfer: anisotropy is independent of vibrational relaxation in the absence of ro-vibrational coupling[12a] and reflects only reorientation. In the present case, since we are using broadband excitation and probing at the same central frequency for the anisotropy measurements, the effect of the coupling, if it exists, will be washed out. However, the peculiar geometry of the sample (section IV in the Supporting Information) will greatly influence the anisotropy measurements. The definition of a magic angle (an angle between the pump and the probe fields for which all rotational contributions are canceled out) is thus questionable.

The raw anisotropy mixes contributions from the thermal and the vibrational states (eq 4 in section I in the Supporting Information). Therefore, its direct interpretation is difficult because it is contaminated by the population relaxation. Nevertheless, around time equal to zero, the thermal contribution is negligible and the raw anisotropy is representative of the orientation of the transition dipole moment. At long delay times, the population has totally relaxed and the raw anisotropy reflects the anisotropy of the thermal contribution. The dynamics of the

(31) (a) Steinel, T.; Asbury, J. A.; Zheng, J.; Fayer, M. D. *J. Phys Chem. A* **2004**, *108*, 10957. (b) Rezus, Y. L. A.; Bakker, H. J. *J. Chem. Phys.* **2005**, *123*, 114502.

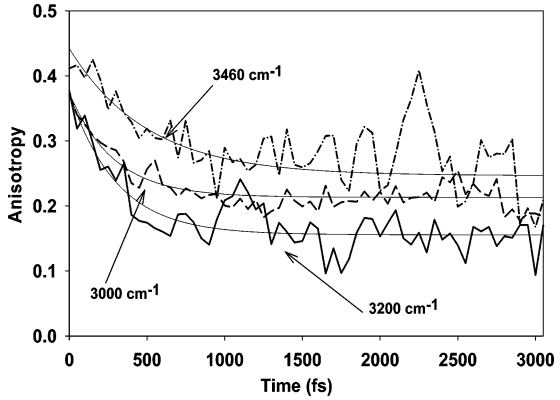

Figure 4. Evolution of the raw anisotropy as a function of the pump frequency (dash−dot line: pump and probe at 3460 cm^{-1}; solid line: pump and probe at 3200 cm^{-1}; dash line: pump and probe at 3000 cm^{-1}). Trend curves [$a \times \exp(-t/\tau) + b$] were added to clarify the figure. From these curves, we get $b = 0.25$ for a pump at 3460 cm^{-1}, $b = 0.15$ for a pump at 3200 cm^{-1}, and $b = 0.21$ for a pump at 3000 cm^{-1}.

raw anisotropy enable us to get additional information on the hydrogen-bond dynamics and the nature of the OH groups on the surface. Figure 4 displays the evolution of the anisotropy as a function of the pump frequency. From this figure, it is clear that there are at least three different species on the surface, exhibiting three different reorientational dynamics. In all three cases, the anisotropy exhibits a plateau at long delay times (i.e., the Heaviside contribution linked to the heating effect). The amplitude of the plateau reflects the available degrees of freedom of the OH vibrator. The higher the plateau value, the lower the number of degrees of freedom. Nevertheless, the mixing of contributions at short delay times prevents the interpretation of the data without care.

The long-term anisotropy is attributed to the thermal state (see above). Since no molecular motions are expected for the physically and chemically sorbed water, once the thermal state is created, the transition dipole moment carrying the ($0 \rightarrow 1$) transition will not rotate anymore. The thermal state anisotropy will then act as a memory function of the nonthermal state anisotropy. The evolution of the thermal anisotropy obeys the following qualitative rule: the higher the thermal anisotropy is, the smaller the amplitude and/or the slower the time constant of the nonthermal anisotropy decay will be.

When pumping−probing at 3460 cm^{-1}, the anisotropy remains high. The high value at long delay times (0.25) is consistent with a highly structured fixed layer of aluminol groups and of adsorbed water on top of them. We thus expect here that the nonthermal anisotropy (see above) will decay slowly and/or partially. We note that this behavior of OH vibrators at an alumina surface is in line with molecular dynamics simulations of adsorbed water in confined silica[32a] and neutron scattering techniques[32b] which have proven that at room temperature interfacial water has a structure similar to that of bulk supercooled water at a temperature of 263 K.

When pumping−probing at 3200 cm^{-1} (water interacting with $AlOH_2^+$ groups), the thermal anisotropy (3 ps) is relatively small (0.15). This is in favor of a system that is losing the memory of its initial excitation. We then expect a rather fast and almost complete decay of the nonthermal anisotropy.

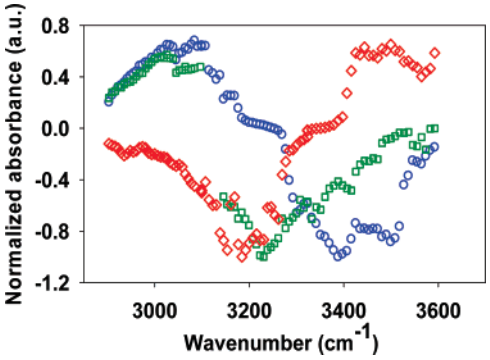

Figure 5. Trends of the pre-exponential factor of the fast contribution (350 fs being the major contribution) according to the pump frequency (blue ○: pump at 3460 cm^{-1}; green □: pump at 3200 cm^{-1}; red ◇: pump at 3000 cm^{-1}). The signals have been normalized with respect to the maximum of the bleaching contribution. In all cases, pump and probe have parallel polarizations.

When pumping−probing at 3000 cm^{-1} ($AlOH_2^+$), the anisotropy remains relatively high (0.21) at long delay times. This intermediate situation indicates that a non-negligible fraction of the thermally excited $AlOH_2^+$ is the initially photoexcited $AlOH_2^+$. Since the $AlOH_2^+$ groups are scarce on the alumina surface, we do not expect a direct excitation transfer from one group to the other.

In Figure 5, we plotted the pre-exponential factor of the fast component of the signal at each pump frequency normalized with respect to the maximum of the bleaching contribution. From that figure, it is clear that this factor is pump frequency dependent. Two types of behavior are depicted in that figure. First, when pumping at 3460 and 3200 cm^{-1}, one observes a bleaching for "high" frequencies while a marked induced absorption is present for "low" frequencies. Those data are consistent with the behavior of water, and their interpretation is described and discussed in the section, "Water Dynamics at the Alumina−Air Interface". Second, when pumping at 3000 cm^{-1}, we observe a bleaching for "low" frequencies and an induce absorption for "large" frequencies. Such a behavior is interpreted in terms of a photoinduced proton transfer and is described and discussed in the section, "Proton-Transfer Dynamics at the Alumina−Air Interface".

Water Dynamics at the Alumina−Air Interface (Pump at 3460 and 3200 cm^{-1}). In the case of a pump at 3460 and 3200 cm^{-1}, Figure 5 shows that, after the pump excitation, the absorption is decreased (bleaching) around the pump frequency corresponding to the ($\upsilon = 0 \rightarrow 1$) transition (due to the ground-state depletion of the probed OH stretching vibration and to stimulated emission; Scheme 2). Moreover, an induced absorption around 3050 cm^{-1} that can be attributed to the ($\upsilon = 1 \rightarrow 2$) transition (due to the excited state populated by the pump; Scheme 2) is observed. Thus, the decay is attributed to the excited-state lifetime of the OH vibrator. The 350-fs mean value for the excited-state lifetime is short compared to the excited lifetime of an isolated OH vibrator (1.3 ps for HOD in D_2O)[12a,b] but comparable, although longer, to the one measured in neat water ($T = 190$ fs).[33]

As shown in Figure 5, the bleaching signals are localized in two separate spectral regions (2900−3300 cm^{-1} on the one

(32) (a) Gallo, P.; Rapinesi, M.; Rovere, M. *J. Chem. Phys.* **2002**, *117*, 369. (b) Bellissent-Funel, M.-C. *J. Phys.: Condens. Matter* **2001**, *13*, 9165.

(33) Cowan, M. L.; Bruner, B. D.; Huse, N.; Dwyer, J. R.; Chugh, B.; Nibbering, E. T. J.; Elsaesser, T.; Miller, R. J. D. *Nature* **2005**, *434*, 199.

Scheme 2. Model Used[a]

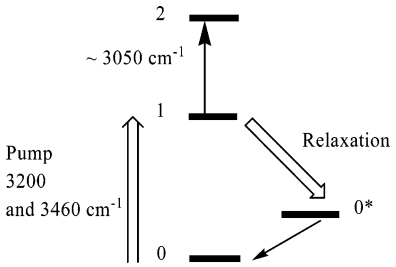

[a] The relaxation of excited OH vibrators from the ($v = 1$) level to the ($v = 0^*$) level was fitted using two time constants: 350 fs (major contribution) and 2.5 ps (minor contribution). The last step in this relaxation pathway is the decay from the ($v = 0^*$) level to the ground state (not observed within the time window of the experiments: Heaviside component).

hand; 3400−3600 cm^{-1} on the other hand). This enables us to deduce that in the probed OH stretching region, there are essentially two spectrally separated OH subensembles that are not coupled to each other: one absorbing in the 2900−3300 cm^{-1} region, and the other absorbing in the 3400−3600 cm^{-1} region.

The anharmonicity of the probed vibrators is measured as the difference between their ground state and their excited-state absorption frequencies. The species absorbing in the 3400−3500 cm^{-1} are characterized by a large anharmonicity (~400 cm^{-1}), whereas it is smaller in the case of physisorbed water interacting with $AlOH_2^+$ groups (~200 cm^{-1} when pumping at 3200 cm^{-1}). An anharmonicity of 300 cm^{-1} has been measured in an HDO/D_2O mixture.[34a] This value has to be compared to the anharmonicity of 100 cm^{-1}, which was measured in non-hydrogen-bonded water molecules:[34b] hydrogen bonds are known to induce large anharmonicities. The results we get are thus consistent with an extended H-bond network on the surface of alumina (i.e., the observed large anharmonicities suggest the presence of H-bonds and thereby a hydrophilic character). Last, the greater anharmonicity (300 cm^{-1})[34a] obtained for the HDO/D_2O mixture than in the case of physisorbed water interacting with $AlOH_2^+$ groups (200 cm^{-1}) may be explained by the strong interactions of the adsorbed water molecules with these acid sites.

The dissociation energy (D_e) of hydroxyl groups of adsorbed H_2O on $AlOH_2^+$ using the framework of the Morse potential (section III in the Supporting Information) is estimated as $D_e = 350 \pm 70$ kJ/mol. The dissociation energy of the O−H bond in water is about 460 kJ/mol in the gas phase.[35] This much smaller value is consistent with the presence of strong hydrogen bonds.

From Figure 4, it is obvious that the anisotropies measured exhibit a fast dynamics. To get an insight into this excited-state dynamics, we have subtracted the spectral components corresponding to the thermal and coherent contributions from both $\Delta\alpha_{\parallel}$ and $\Delta\alpha_{\perp}$ (section II in the Supporting Information): the components corresponding to the excited-state lifetime (350 fs and 2.5 ps) are thus considered (Scheme 2). The subtraction procedure assumes that the vibrational excited-state relaxation gives rise to an instantaneous appearance of the hot ground state (i.e., there are no intermediates in the relaxation pathway of the vibrational excited state toward the hot ground state). The anisotropies obtained are displayed in Figure 6. The different decays have been fitted with a single exponential decay [$a \times \exp(-t/\tau) + b$]. The fitted values are $\tau = 400$ fs, $a = 0.2$, and $b = 0.3$ for a pump at 3460 cm^{-1} and $\tau = 400$ fs, $a = 0.45$, and $b = 0.05$ for a pump at 3200 cm^{-1}. It is clear that these time constants are not consistent with the value attributed to orientational dynamics of bulk water molecules ($\tau_{OR} = 2.6$ ps).[31b,36]

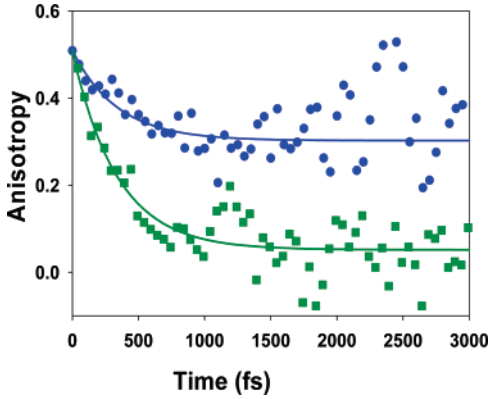

Figure 6. Evolution of the anisotropy after subtraction of the spectral component corresponding to the thermal and coherent contributions from both $\Delta\alpha_{\parallel}$ and $\Delta\alpha_{\perp}$ as a function of the pump frequency (blue ●: pump and probe at 3460 cm^{-1}; green ■: pump and probe at 3200 cm^{-1}). The decays have been fitted with a single exponential decay ($a \times \exp(-t/\tau) + b$; see Supporting Information). The fitted values are $\tau = 400 \pm 100$ fs, $a = 0.2$, and $b = 0.3$ for a pump at 3460 cm^{-1} and $\tau = 400 \pm 100$ fs, $a = 0.45$, and $b = 0.05$ for a pump at 3200 cm^{-1}.

When pumping at 3460 and 3200 cm^{-1}, the initial anisotropy just after the excitation reaches a value of 0.5, which is greater than the 0.4 value expected for isotropic media. These unusual values are in fact just the consequence of the anisotropic nature of the sample. For such samples, it is extremely hazardous to rationalize the initial amplitude (0.5) of the data with the scheme usually used for isotropic media such as liquids, micelles, and so forth. Furthermore, we have no information on the local orientational distribution of the OH vibrators that will have a dramatic influence on the expected anisotropy. In section IV in the Supporting Information, we calculated the anisotropy for a simple model of isolated AlOH groups that demonstrates (i) an anisotropy of 0.4 for a perfectly aligned system of nanotubes and (ii) an anisotropy that can be as high as 1 for a system of transverse nanotubes. It is thus not surprising to get an anisotropy value greater than 0.4 in these anisotropic samples.

When pumping−probing at 3200 cm^{-1}, the anisotropy decay is nearly complete. This can be explained by an intermolecular energy transfer described by dipole−dipole interactions (i.e., the Förster transfer mechanism as introduced by Woutersen and Bakker to explain the loss of anisotropy as a function of the H/D ratio in neat liquid water).[37] However, we cannot exclude additional mechanisms based on intermolecular anharmonic interactions involving strong hydrogen bonds. It is clear that the associated anisotropy decay time constant at all pump frequencies is longer than that in bulk water ($\tau_{3D} = 75$ fs).[33] The higher time constant ($\tau_{2D} = 400$ fs) obtained in the present experiments reflects the change of the dimensionality of the

(34) (a) Bakker, H. J.; Nienhuys, H.-K. *Science* **2002**, *297*, 587. (b) Graener, H.; Seifert, G. *J. Chem. Phys.* **1993**, *98*, 36.
(35) Herzberg, G. *Molecular Spectra and Molecular Structure;* Krieger Publishing: Malabar, FL, 1989; Vol. I, reprinted.
(36) Piletic, I. R.; Moilanen, D. E.; Spry, D. B.; Levinger, N. E.; Fayer, M. D. *J. Phys. Chem. A* **2006**, *110*, 4985.
(37) Woutersen, S.; Bakker, H. J. *Nature* **1999**, *402*, 507.

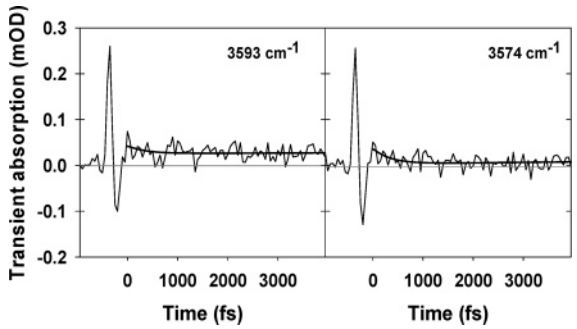

Figure 7. Transient absorption kinetics recorded for a pump at 3000 cm^{-1} and a single channel detection at 3593 cm^{-1} (left) and at 3574 cm^{-1} (right). The bold lines are trend curves added to clarify the reading. Gray lines indicate the zero level. Note the presence at negative delay times of a signal due to free induction decay. Pump and probe have parallel polarizations.

energy-transfer mechanism: going from 3D in bulk water to 2D for surface water. The fact that the anisotropy does not decay to zero indicates also that the H-bond network around the excited water molecules is not totally randomly oriented.

When pumping−probing at 3460 cm^{-1} (AlOH groups and physisorbed H_2O), the time constant remains the same within the error bars as in the case of adsorbed water on $AlOH_2^+$. However, the residual anisotropy is greatly increased (0.3 compared to 0.05), as expected for a highly structured environment (Scheme 1). Indeed, if energy is transferred between aligned OH groups, then the corresponding anisotropy will be less affected. Therefore, the data support the idea of well-packed AlOH groups and H_2O patches on the surface as presented in Scheme 1.

Proton-Transfer Dynamics at the Alumina−Air Interface (Pump at 3000 cm^{-1}). The behavior depicted in Figure 5 is completely different when pumping at 3460 and 3200 cm^{-1} as compared to that when pumping at 3000 cm^{-1}. In the latter case, we observe a bleaching not around the pump frequency but instead around 3175 cm^{-1}, corresponding to water interacting with $AlOH_2^+$ sites. There is no obvious excited-state absorption in the red region. It is worth noting that the preexponential factor of the fast component is positive between 3450 and 3550 cm^{-1} (i.e., in the AlOH spectral region). This might be explained by a photoinduced proton transfer from $AlOH_2^+$ to its neighboring water molecule according to eq 1:

$$AlOH_2^+ + H_2O \underset{\text{back-transfer}}{\overset{h\nu}{\rightleftharpoons}} AlOH + H_3O^+ \qquad (1)$$

Such a reaction would induce a bleaching around 3200 cm^{-1} (water molecule around the excited $AlOH_2^+$), a bleaching around the pump frequency, as well as an absorption above 3500 cm^{-1} (AlOH) and around 3000 cm^{-1} (H_3O^+).[38]

To verify such a hypothesis, in Figure 7 we plotted the transient absorption kinetics in the blue wing of the spectral window (AlOH region). These kinetics clearly exhibit a positive induced absorption for positive delay times. In that spectral region (around 3550−3600 cm^{-1}), only aluminol groups have a significant extinction coefficient and are thus responsible for this positive absorption. That is in favor of eq 1, which implies the ultrafast (below the time resolution of the experimental setup) formation of aluminol groups. In the spectral region

Scheme 3. Model Used in the Case of the Pump at 3000 cm^{-1}

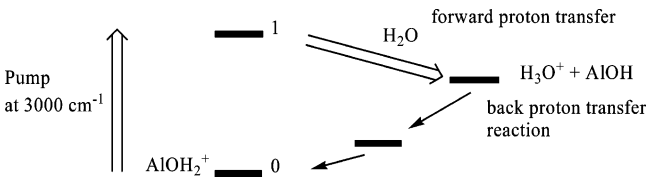

around 3000 cm^{-1}, the situation is less clear because of the interplay between the extinction coefficients of H_3O^+, $AlOH_2^+$, and H_2O species. As a result, only a weak signal is detected around 3000 cm^{-1}.

Moreover, we note that the induced absorption in Figure 7 does not decay to zero. This indicates that even after a long delay time (3 ps), the acid−base equilibrium between aluminol and $AlOH_2^+$ groups is shifted toward the formation of aluminol groups and hydronium ions.

The kinetics plotted in Figure 2a exhibits the evolution of the water molecules involved in eq 1. Within the time resolution of the setup, the bleaching arises from the consumption of water molecules involved in eq 1. The recovery of the bleaching is the result of the back proton-transfer reaction (i.e., the reformation of $AlOH_2^+$ from aluminol groups and hydronium ions) that is presently fitted as the sum of two components at 350 fs (major contribution) and 2.5 ps (minor contribution). This back proton-transfer reaction has thus a mean time constant of 350 fs.

Recent studies[39] on the proton transfer in liquid water and in particular on the equilibrium between the Eigen ($H_9O_4^+$) and the Zundel form ($H_5O_2^+$) of the hydrated proton have shown that the Eigen form relaxes toward the Zundel one extremely quickly (<100 fs)[39a] and that the lifetime of the excited proton is short (120−170 fs).[39] Within our spectral range and time resolution (200 fs), we could not observe any excited-state absorption, either for AlOH groups or for hydrated protons involved in eq 1. This might be explained either by an ultrafast relaxation, as proven in the case of the hydrated proton,[39] or by the endothermic character of eq 1. As a consequence, it is possible to probe the ground-state dynamics of the proton in the red spectral region (around 3000 cm^{-1}; Scheme 3).

To get an insight into the nonthermal anisotropy, we subtracted the spectral components corresponding to the thermal and coherent contributions from both $\Delta\alpha_{\parallel}$ and $\Delta\alpha_{\perp}$ (section II in the Supporting Information).

When pumping−probing at 3000 cm^{-1} (Figure 8), the anisotropy decay is slow (900 fs) and complete within the error bars of the experiment. As stated earlier, this time constant is not consistent with the value attributed to orientational dynamics of bulk water molecules (τ_{OR} = 2.6 ps).[31b,36] In our case, the delocalized excited vibrational states of the OH stretching vibrator induce a proton transfer within the O−H···O system[34a] (eq 1). Once the proton is transferred to one of the neighboring water molecules, the proton can either hop within the H-bond network or be back-transferred to the surface. We have shown that the mean time constant of this back-transfer is 350 fs. The fact that the anisotropy decays to zero can be attributed either to a complete rotational dynamics or to a hopping process exploring all the possible configurations. Since water molecules

(38) (a) Giguère, P. A.; Turrell, S. *Can. J. Chem.* **1976**, *54*, 3477. (b) Librovich, N. B.; Sakun, V. P.; Sokolov, N. D. *Chem. Phys.* **1979**, *39*, 351.

(39) (a) Woutersen, S.; Bakker, H. J. *Phys. Rev. Lett.* **2006**, *96*, 138305. (b) Amir, W.; Gallot, G.; Hache, F.; Bratos, S.; Leicknam, J.-C.; Vuilleumier, R. *J. Chem. Phys.* **2007**, *126*, 034511.

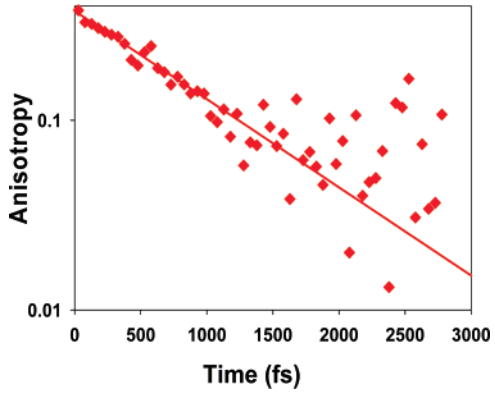

Figure 8. Evolution of the anisotropy after subtraction of the spectral component corresponding to the thermal and coherent contributions from both $\Delta\alpha_{\parallel}$ and $\Delta\alpha_{\perp}$ for a pump and probe at 3000 cm^{-1} using a logarithm scale (red ◆). The decay has been fitted with a single exponential decay ($a \times \exp(-t/\tau) + b$; see section II in the Supporting Information). The fitted values are $\tau = 900 \pm 100$ fs, $a = 0.38$, and $b = 0.0$.

are attached to the surface, their motions are restricted. Therefore, the anisotropy decay we observe is due to another mechanism, which is possibly the coupled hopping process of a hydronium ion and a water molecule through eq 2. We may note that this implies a locally extended H-bond network.

$$H_3O^+ + H_2O \xrightarrow{\text{H-bond network}} H_2O + H_3O^+ \qquad (2)$$

The anisotropy at 3000 cm^{-1} probes the loss of anisotropy due to (i) the missing $AlOH_2^+$, (ii) the missing water molecule, and (iii) the hydrated proton (eq 1). Among those species, only the water and the hydrated proton are involved in a dynamical equilibrium (eq 2), once the forward proton-transfer reaction is achieved (eq 1). Let us note that an anisotropy experiment will be sensitive to the global proton hopping and not to the Eigen−Zundel equilibrium since the latter is characterized by a time constant smaller than 100 fs[39a] (faster than the time resolution of the present setup). A proton jump (eq 2) will induce a change of anisotropy because the consumed and formed water molecules (and the consumed and formed hydrated protons) will have different directions for their transition moments. If the accessible H-bond network for the hydrated proton is large enough, the anisotropy will be totally lost after a few jumps.

The measured decay time for the anisotropy at 3000 cm^{-1} (900 fs) might thus be attributed to the hopping time for the proton transfer. This proposed time is consistent with recent studies on proton transfer in water[39] which support the idea of a proton jump within the picosecond time range. Moreover, our proposed value is consistent with ∼1-ps time calculated using molecular dynamics[40a] and ∼1.5-ps time obtained by NMR measurements.[40b]

Conclusion

It is quite complex to characterize and describe the γ-alumina surface. Nevertheless, temperature difference FT-IR spectra together with literature data[3] enable us to assign the different bands present in the O−H stretching region. Moreover, pump−probe IR−IR femtosecond measurements allow us to get a local point of view of the surface. These two pictures are consistent: on the one hand, water molecules ($AlOH_2^+$ groups and surrounding water molecules) are respectively studied when pumping at 3000 and 3200 cm^{-1}; on the other hand, physisorbed water as well as aluminol groups are certainly responsible for the large bleaching between 3400 and 3500 cm^{-1} when pumping at 3460 cm^{-1} (Figure 5). As the molecules under study are "frozen" on the surface on the time scale of the experiments (a few picoseconds), the anisotropy relaxation is not due to molecular reorientation but instead to energy transfer (by means of strong dipole−dipole interactions in the case of a pump at 3460 and 3200 cm^{-1}) and to proton transfer (in the case of a pump at 3000 cm^{-1}). Thermal gravimetric experiments prove that there is roughly one layer of physisorbed water on the surface. Therefore, the H-bond network is limited and fewer degrees of freedom are available than in the case of neat water.

For physisorbed water and aluminol groups, the vibrational excited-state lifetime is found to be 350 ± 50 fs. The 350-fs mean value for the excited-state lifetime is short compared to the excited lifetime of an isolated OH vibrator (1.3 ps for HOD in D_2O)[12a,b] but comparable, although longer, to the one measured in neat water ($T = 190$ fs).[33] The strong decrease in the degrees of freedom accounts also for the differences between the time constants associated with the decay of anisotropy in pure water ($\tau_{3D} = 75$ fs)[33] and in our case ($\tau_{2D} = 400$ fs). The ratio of the time constants associated with the anisotropy in the case of neat water and in the case of surface water is $\tau_{2D}/\tau_{3D} \approx 5$. This ratio reflects the change of dimensionality in the energy transfer and the specificity of surface chemistry. The limited H-bond network explains why we observe a partial decay of anisotropy when pumping at 3460 and 3200 cm^{-1} (Figure 6), as not all possible orientations are available for the OH vibrators. The results are consistent with the presence of well-packed aluminol groups (characterized by a high residual anisotropy), a H-bond network of physisorbed water (the residual anisotropy is almost vanishing), and a locally extended H-bond network around the Brønsted acid sites (as no residual anisotropy is observed in this case; Figure 8).

Interestingly, the femtosecond results evidence an IR-induced proton-transfer reaction (eq 1) on the surface. The back proton-transfer reaction is also observed. We measure the reaction time constant of an aluminol with a hydronium ion (350 ± 50 fs). We stress that the fact that the time constant for the back proton-transfer reaction (eq 1) and the excited-state lifetime of the O−H vibrator (water molecules and AlOH groups) are more or less equal is coincidental. The proposed characteristic hopping time of the proton (900 ± 100 fs) is in line with the theoretical predictions and NMR measurements in liquid water.

The alumina surface is characterized by microheterogeneities that influence the physical and chemical properties of adsorbed water. Even though adsorbed water can obviously be described as frozen (no molecular motions are detected on the picosecond time scale), we observe the required strong dipole−dipole coupling (evidenced by the excitation propagation mechanism), the locally extended H-bond network, and the proton-transfer channels necessary for a rich surface chemistry.

Acknowledgment. Laserlab Europe is gratefully acknowledged for financial support under Contracts RII3-CT-2003-506350 and MTKD-CT-2004-509761. Eurolabo (Hellma France) is gratefully acknowledged for making temperature difference FT-IR experiments possible. We thank Mickaël Dollé for his help in TGA measurements. We are thankful to the authors of

(40) (a) Vuilleumier, R.; Borgis, D. *J. Chem. Phys.* **1999**, *111*, 4251. (b) Meiboon, S. *J. Chem. Phys.* **1961**, *34*, 375.

ref 39b for giving us their results before publication. We thank Thomas Gustavsson for helpful discussions. Sylvie Poissonnet and Patrick Bonnaillié are gratefully acknowledged for SEM images.

Supporting Information Available: Presentation of the raw anisotropy (section I), the procedure to subtract both the coherent and the long-lived contributions from the data (section II), the expression of the dissociation energy using the framework of the Morse potential with a focus on physisorbed water interacting with $AlOH_2^+$ groups (section III), and the calculation of anisotropy for isolated aluminol AlOH groups in an anisotropic system of parallel nanotubes (section IV). This material is available free of charge via the Internet at http://pubs.acs.org.

JA0691730